Chinese Journal of Natural Medicines

Expanding molecular diversity of ribosomally synthesized and post-translationally modified peptide (RiPP) natural products by radical S-adenosylmethionine (SAM) enzymes: recent advances and mechanistic insights

Jiawei Feng, Jiarong Mo, Xinya Hemu

Citation: Jiawei Feng, Jiarong Mo, Xinya Hemu, Expanding molecular diversity of ribosomally synthesized and post-translationally modified peptide (RiPP) natural products by radical S-adenosylmethionine (SAM) enzymes: recent advances and mechanistic insights, Chinese Journal of Natural Medicines, 2025, 23(3), 257-268. doi: 10.1016/S1875-5364(25)60845-4.

View online: https://doi.org/10.1016/S1875-5364(25)60845-4

Chinese Journal of Natural Medicines 23 (2025) 257-268

Contents lists available at ScienceDirect

Chinese Journal of Natural Medicines

journal homepage: www.cjnmcpu.com/

Review

Expanding molecular diversity of ribosomally synthesized and post-translationally modified peptide (RiPP) natural products by radical S-adenosylmethionine (SAM) enzymes: recent advances and mechanistic insights

Jiawei Feng, Jiarong Mo, Xinya Hemu*

State Key Laboratory of Natural Medicines, School of Traditional Chinese Pharmacy, China Pharmaceutical University, Nanjing 210098, China

ARTICLE INFO

Article history:
Received 25 June 2024
Revised 20 August 2024
Accepted 10 September 2024
Available online 20 March 2025

Keywords:
Ribosomally synthesized and post-translationally modified peptides
Radical S-adenosylmethionine
Epimerization
Methylation
Side-chain cross-linking

ABSTRACT

Ribosomally synthesized and post-translationally modified peptides (RiPPs) constitute a vast and diverse family of bioactive peptides. These peptides, synthesized by ribosomes and subsequently modified by various tailoring enzymes, possess a wide chemical space. Among these modifications, radical S-adenosylmethionine (rSAM) enzymes employ unique radical chemistry to introduce a variety of novel peptide structures, which are crucial for their activity. This review examines the major types of modifications in RiPPs catalyzed by rSAM enzymes, incorporating recent advancements in protein structure analysis techniques and computational methods. Additionally, it elucidates the diverse catalytic mechanisms and substrate selectivity of these enzymes through an analysis of the latest crystal structures.

1. Introduction

Ribosomally synthesized and post-translationally modified peptides (RiPPs) represent an increasingly diverse class of natural products. Their extensive modifications confer a variety of chemical scaffolds, diverse biological activities, and generally enhanced molecular stability, presenting significant potential for drug development [1, 2]. The well-studied lanthipeptide nisin, derived from bacteria, exemplifies this potential, demonstrating antimicrobial activity and utility in preventing the growth of foodborne pathogens [3]. Darobactin, a potent antibiotic produced by *Photorhabdus khanii*, exhibits strong inhibitory activity against several clinically relevant Gram-negative resistant bacteria. It achieves this by binding with high affinity to the bacterial outer membrane protein BamA, thereby inhibiting outer membrane assembly [4]. The fungal-derived multicore peptide dikaritin inhibits microtubule assembly and mitosis in human tumor cells at low micromolar concentrations, demonstrating antitumor activity [5]. Astins from *Aster tataricus* endophyte have been shown to have hepatotoxic effects [6]. Toxin peptides from animal venoms, including those from marine cone snails, spiders, scorpions, toads, and snakes, specifically target different ion channels and neural receptors. These peptides offer promising therapeutic potential in the treatment of chronic pain, cardiovascular diseases, and psychiatric disorders [7-16]. Plant-derived cyclic peptides, such as the first discovered cyclotide kalata B1, exhibit exceptionally high stability against heat and chemical stress, showing anthelmintic properties against parasitic pathogens [17]. Additionally, bicyclic octapeptide moroidins demonstrate broad-spectrum antimitotic activities [18-20].

The intricate chemical structures of RiPPs necessitate the elucidation of biosynthetic pathways and the identification of associated enzymes for their practical applications. RiPP precursor peptides are generally understood to comprise two components: a leader peptide and a core peptide [21, 22]. Post-translational modification (PTMs) enzymes recognize the leader peptide to modify the core peptide, executing various modifications followed by the proteolytic release of the mature peptides [23-29]. In these post-translational modification processes, radical S-adenosyl-L-methionine (rSAM) enzymes, an emerging superfamily of metalloenzymes, play a crucial role in expanding the structural diversity of RiPP peptidyl scaffolds (Fig. 1) [30-35].

The rSAM enzymes are characterized by their distinctive radical initiation mechanism involving a SAM group. All enzymes in the rSAM family exhibit a characteristic rSAM domain in a $(\beta/\alpha)_6$ partial TIM (triose phosphate isomerase) barrel [36] structure comprising of 6α-helices and 6β-strands (Fig. 2). A minimum of one [4Fe-4S] cluster is coordinated and stabilized by cysteines in a conserved CxxxCxxC motif at the center of the TIM barrel, playing a crucial role in electron transfer. This rSAM iron-sulfur (RS) cluster coordinates bidentately with both the carboxyl and amino groups of SAM [37]. The radical-based reactions catalyzed by rSAM enzymes typically commence with the reductive cleavage of SAM to generate L-methionine and a 5'-deoxyadenosyl radical (5'-dA•). Research suggests that this process involves the formation

* Corresponding author.
E-mail address: hemuxinya@cpu.edu.cn

https://doi.org/10.1016/S1875-5364(25)60845-4

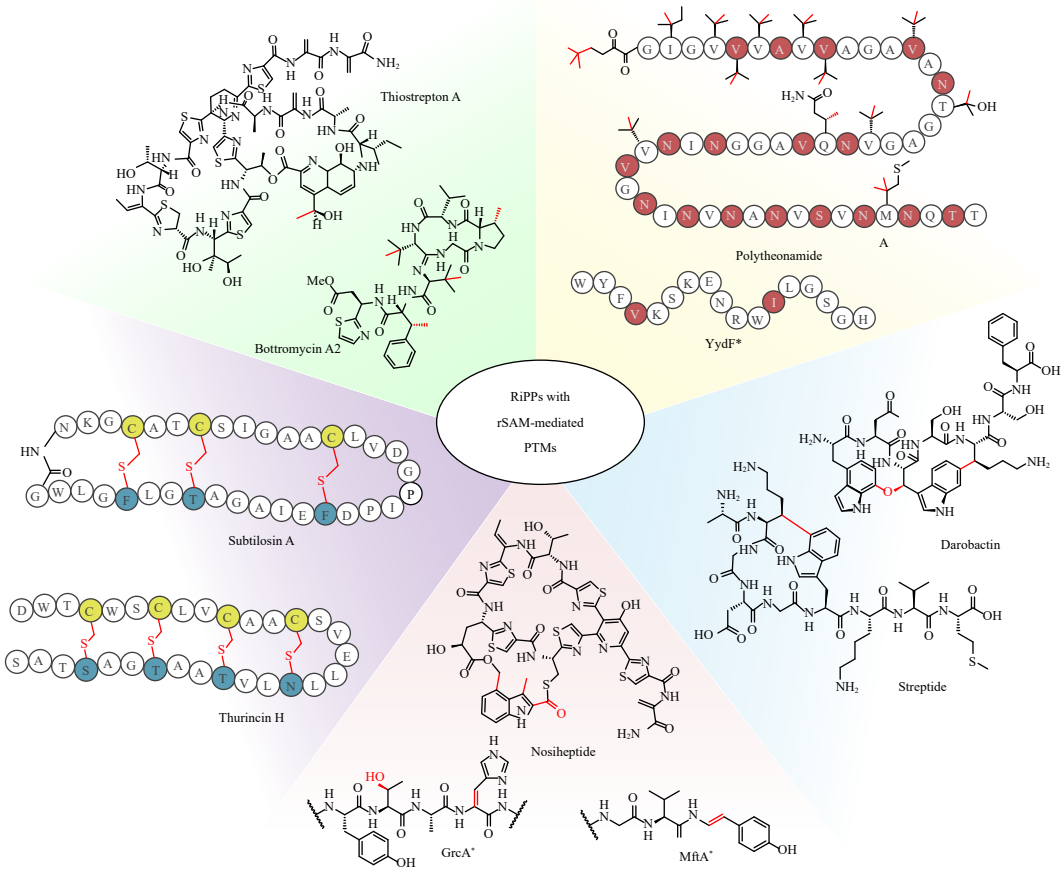

Fig. 1 Representative rSAM-catalyzed RiPP natural products. Structures of the representative molecules with rSAM-mediated epimerization, methylation, thioether-formation, C-X cross-linking, and other modifications (oxidation and rearrangement) are presented with distinct background colors: yellow, green, purple, blue, and pink, respectively. Red spheres indicate epimerized residues, while yellow spheres and blue spheres denote donor and acceptor sites forming thioether bonds, respectively. Bonds formed *via* rSAM-catalyzed reactions are highlighted in red. *Represents peptide precursor with post-translational modifications.

of an organometallic intermediate Ω *via* rearrangement [38, 39]. Subsequently, the 5'-dA• abstracts a hydrogen atom from the substrate, yielding 5'-deoxyadenosine (5'-dA) and a substrate radical intermediate. This intermediate can proceed through various reaction pathways, resulting in a diverse array of modified products, including epimerization [40], methylation [24, 25], thioether formation [41, 42], C-C/C-heteroatom cross-linking [26, 43], as well as oxidation [29, 44] and rearrangement [45]. Furthermore, studies have revealed that some rSAM enzymes possess extended domains at their N- or C-termini, such as the cobalamin-binding domain (CBD) [46] and the SPASM/Twitch domain [47]. The latter is named after its founding members: subtilosin A, pyrroloquinoline quinone (PQQ), anaerobic sulfatase, and mycofactocin. These extended domains can bind other cofactors, including pyridoxal phosphate and cobalamin, or additional auxiliary iron-sulfur clusters (Auxiliary cluster, Aux).

Bioinformatics tools for mining microbial genome data are essential in discovering and identifying rSAM enzymes. These computational approaches significantly enhance the efficiency and effectiveness of uncovering natural peptides with unique structures compared to traditional methods of extraction, isolation, or serendipitous discovery. For example, in 2018, Mohammad et al. [48] successfully mapped gene clusters of streptococcal rSAM-RiPPs natural products, identifying several novel scaffold-modified RiPPs peptides. In 2022, Li et al. [49] developed the SPECO tool based on the co-occurrence and co-conservation synthesis logic of RiPPs, enabling the characterization of three new rSAM-mediated side-chain cross-linked cyclic peptides. Currently, databases contain approximately 770 000 rSAM enzyme records (as of June 2024), yet less than 1% have been experimentally characterized (Table 1) [50]. To elucidate the contributions of rSAM enzymes to the diversity of RiPP natural products, this review integrates insights from the classification, structure, and catalytic mechanisms of four types of rSAM-catalyzed reactions, combining the recent advances in biochemical, spectroscopic, bioinformatics, crystallographic, and computational simulation techniques.

2. Epimerization

Genetically encoded proteins exhibit a strong preference for L-amino acids, while radical SAM (rSAM) enzymes enhance the chemical complexity of RiPPs by introducing D-amino acids. In the biosynthesis of proteusins [23] and epipeptides [51], two classes of D-amino acid-containing RiPPs, a series of rSAM enzymes are identified in the biosynthesis gene clusters to catalyze the *α*-C epimerization of the backbone residues (Fig. 3A). The catalytic cycle commences with the cleavage of SAM, generating a 5'-dA• that abstracts a hydrogen atom from the *α*-C atom of the peptide residue, forming 5'-dA and a peptide radical intermediate centered on the *α*-C. This radical intermediate subsequently receives hydrogen from the thiol of a cysteine residue in the rSAM enzyme, producing the epimerized peptide product, while the thiol of the cysteine residue in the enzyme becomes a sulfur radical. The sulfur radical intermediate is then reduced back to the thiol of the cysteine residue, preparing it for the next catalytic cycle.

The marine sponge *Theonella swinhoei* hosts numerous uncultivated bacterial symbionts, representing a rich source of bioactive metabolites. Among these are the structurally complex and potent peptide natural toxins polytheonamide A and B, the initial members of the proteusin class of RiPPs [23]. Research has re-

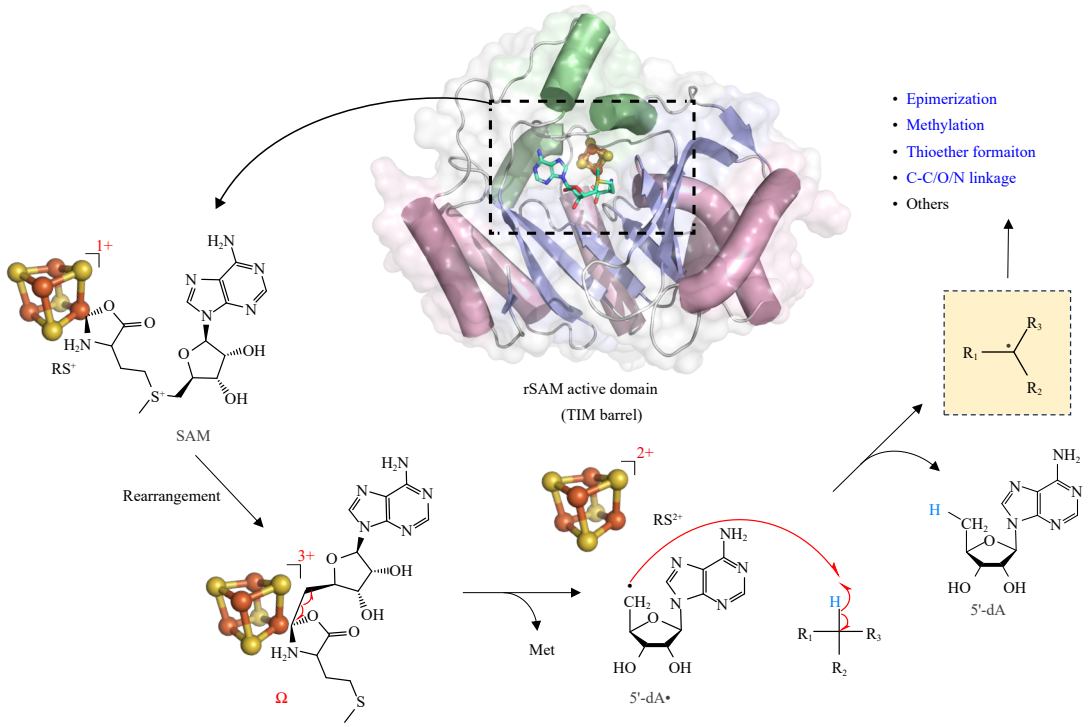

Fig. 2 General mechanism of rSAM enzyme-catalyzed radical reactions. The electron transfer within the rSAM cluster facilitates the reductive cleavage of SAM, forming a rearranged intermediate Ω. The released 5'-dA• abstracts a hydrogen atom from the substrate, generating a substrate radical intermediate. This intermediate subsequently follows diverse reaction pathways, undergoing various modifications.

vealed that these peptides contain 18 non-natural D-amino acids within their 49 residues. Biochemical characterization has confirmed that the rSAM enzyme PoyD, encoded downstream of their precursor peptide gene, is responsible for the epimerization of these 18 residues. This epimerization occurs in a directed (conversion from L- to D-configuration) and spaced manner, progressing with directionality from the *C*-terminus to the *N*-terminus [27]. Furthermore, PoyD catalyzes a wide range of substrate residues, including Val, Ala, Asn, Ser, and Thr. The cysteine residue at position 372 in PoyD functions as a critical hydrogen donor, providing a hydrogen atom from the opposite side of the substrate to generate the epimerized product. The cysteine is converted to a sulfur radical, which is subsequently reduced to enter the next catalytic cycle (Fig. 3B). While the precise mechanism remains incompletely understood, it is hypothesized to involve assistance from other residues, similar to ribonucleotide reductase or spore photoproduct lyase [52-54].

Several rSAM enzymes [55] are involved in proteusin modification. OspD, isolated from the cyanobacterium *Oscillatoria* sp. PCC 6506 [56], catalyzes the epimerization of Val and Ile residues in the precursor peptide OspA. AvpD, found in *Anabaena variabilis* ATCC 29413 [57], is responsible for the epimerization of three Phe residues in the precursor peptide AvpA. PlpD, identified in *Pleurocapsa* sp. PCC 7319 [58], operates on three encoded precursor peptides (plpA1, A2, A3), catalyzing the epimerization of Val and Ile in A1, Ser in A2, and Met in A3. A recent discovery revealed carnazolamide, a highly modified peptide from *Chryseobacterium carnipullorum* DSM 25581, representing a new subfamily of proteusins [59]. In this organism, the rSAM enzyme CcaD catalyzes the epimerization of L-Pro in the peptide. Experimental data indicates that this reaction occurs subsequent to the completion of other post-translational modifications.

Epipeptides represent another class of RiPPs that undergo Cα epimerization [60]. In *Bacillus subtilis*, the yydFGHIJ operon encodes ribosomally synthesized peptides containing D-amino acids, which play a crucial role in inducing the expression of the LiaRS two-component system that triggers the bacterial cell membrane stress response [51, 61]. The epimerization process occurs at positions Val36 and Ile44 in the YydF precursor peptide, catalyzed by the standalone rSAM enzyme YydG. Unlike PoyD, YydG is predicted to possess a SPASM domain in its structure, coordinating an additional [4Fe-4S] cluster. Similar to PoyD, Cys223 in YydG is presumed to act as a hydrogen donor. However, the resulting sulfur radical is stabilized not by assistance from other residues but by the additional [4Fe-4S] cluster in the SPASM domain, forming a five-coordinate iron with unique properties that facilitate radical quenching (Fig. 3B).

A distinctive characteristic separating proteusin-class RiPPs from others is the presence of a conserved nitrile hydratase-like leader peptide at the *N*-terminus of proteusin precursors, resulting in larger precursors (exceeding 150 amino acids). This conserved sequence is absent in the YydF-encoded precursor, leading Olivier Berteau and colleagues to designate this peptide as an epipeptide. Comparative analysis of rSAM enzymes from proteusins, epipeptides, and other known RiPP-modifying rSAM enzymes reveals that YydG lacks the RiPP precursor recognition element (RRE/PqqD domain) commonly found in rSAM enzymes. This observation suggests that YydG has evolved independently from other rSAM epimerases, a hypothesis supported by experimental evidence demonstrating that a truncated YydF precursor remains reactive with YydG.

Recently, the crystal structure of the complex between YydG (hereafter referred to as EpeE) and the substrate peptide segment has been elucidated (PDB code: 8AI2) [62]. The structure reveals that the Cα atom of residue Ile44 of the modified precursor peptide is positioned 3.8 Å from the C5' atom of SAM, optimally situated for direct hydrogen abstraction by 5'-dA• (Fig. 3C). Concurrently, the conserved cysteine residue C223 is located below Ile44, acting as a critical hydrogen donor. Following hydrogen atom abstraction from the substrate residue, C223 facilitates the quenching of the substrate radical intermediate, resulting in a conformational change and the formation of a transient sulfur radical intermediate. Additionally, D210 not only provides structural stabilization for C223 but also supplies a proton for the re-

Table 1 Representative RiPPs with post-translational modifications involving rSAM enzymes

PTM	RiPP class	Example	Radical SAM	Bacteria origin	Activity/Function
Epimerization	Proteusin	Polytheonamide A	PoyD [27]	*Theonella swinhoei* (strain pTSMAC1)	Cytotoxic
		OspA	OspD [56]	*Kamptonema* sp. PCC 6506 (*Oscillatoria* sp.)	Unknown
		AvpA	AvpD [57]	*Trichormus variabilis* ATCC 29413 (*Anabaena variabilis*)	Unknown
		PlpA1, A2, A3	PlpD [58]	*Pleurocapsa* sp. PCC 7319	Unknown
		Carnazolamide	CcaD [59]	*Chryseobacterium carnipullorum* DSM 25581	Unknown
	Epipeptide	YydF/EpeX	YydG (EpeE) [51]	*Bacillus subtilis* (strain 168)	Antimicrobial, cell envelope stress response
	GRC	GrcA	GrcC [44]	*Streptococcus pneumoniae* A 34562	Unknown
Methylation	Proteusin	Polytheonamide A	PoyB, PoyC [69, 70]	*Theonella swinhoei* (strain pTSMAC1)	Cytotoxic
	Bottromycin	Bottromycin A2	BotRMT1-3 [71]	*Streptomyces* sp. BC 16019	Antibacterial
	Thiopeptide	Thiostrepton A	TsrM (TsrT) [72, 73, 75]	*Streptomyces laurentii*	Antibacterial, antimalarial, anticancer
		Nosiheptide	NosN [76]	*Streptomyces actuosus* ATCC 25421	Antibacterial
		Thiomuracin	TbtI [79, 80]	*Thermobispora bispora*	Antibacterial
C-C/O/N cross-link	Streptide	Streptide	StrB [26]	*Streptococcus thermophilus* LMD-9	Unknown
			SuiB [104, 105]	*Streptococcus suis* 92-4172	
	Ryptide	RrrA	RrrB [103]	*Streptococcus suis* LSS38_2	Unknown
	ITF	ItfA	ItfD [102]	*Bacteroides thetaiotaomicron*	Unknown
	Daropeptide	Darobactin	DarE [43]	*Photorhabdus khanii* HGB 1456	Antibacterial
	Rotapeptide	TqqA	TqqB [106]	*Streptococcus suis* R 735	Unknown
	Bicyclostreptin	Bicyclostreptin A	HghB, HghC [114]	*Streptococcus thermophilus* JIM 8232, *S. agalactiae* MRI Z1-218	Growth regulation
Thioether cross-link	Sactipeptide	Subtilosin A	AlbA [95]	*Bacillus subtilis* 168	Antibacterial
		Thurincin H	ThnB [84]	*Bacillus thuringiensis* SF 361	Antibacterial
		Thuricin CD (Trn-α, Trn-β)	TrnC, TrnD [85, 86]	*Bacillus thuringiensis* DPC 6431	Antibacterial
		Sporulation killing factor	SkfB [88]	*Bacillus subtilis*	Antibacterial
		Thuricin Z (Huazacin)	ThzC, ThzD [90]	*Bacillus thuringiensis*	Antibacterial
		Ruminococcin C	RumMC1, RumMC2 [91-93]	*Ruminococcus gnavus* E1	Antibacterial
		Streptosactin	GggB [94]	*Streptococcus thermophilus* JIM 8232	Antibacterial
		Thermocellin	CteB [100]	*Clostridium thermocellum* ATCC 27405	Unknown
	Ranthipeptide	Freyrasin	PapB [82]	*Paenibacillus polymyxa* ATCC 842	Unknown
		NxxC	NxxcB [99]	*Streptococcus orisratti*, *S. porci*	Unknown
Oxidation/Rearrangement	GRC	GrcA	GrcD [44]	*Streptococcus pneumoniae* A 34562	Unknown
	Mycofactocin	Mycofactocin	MftC [29]	*Mycobacterium tuberculosis*	Primary alcohol metabolism, Growth regulation
	Thiopeptide	Nosiheptide	NosL [45]	*Streptomyces actuosus* ATCC 25421	Antibacterial

generation of the thiol group.

Most rSAM enzymes catalyze the α-C epimerization of peptides. Recently, rSAM-catalyzed epimerization at the inert β position has been discovered. In the pathogen *Streptococcus pneumoniae* A 34562, which causes bacterial pneumonia, a biosynthetic gene cluster *grc* encoding RiPPs associated with quorum sensing regulation has been identified [44]. Two genes encoding rSAM enzymes, GrcC and GrcD, are located in proximity to the precursor coding gene. Experimental evidence demonstrates that GrcC catalyzes the epimerization of L-Thr at the β-C position, resulting in L-allo-Thr formation. Further investigation is required to elucidate the mechanism of epimerization at the Cβ position.

3. Methylation

Methylation reactions are widely recognized for their ubiquity and significance in biological systems. The majority of these reactions employ SAM as the methyl donor [63], proceeding *via* an SN2 bimolecular nucleophilic substitution mechanism [64], which necessitates nucleophilic substrates. However, nature has also

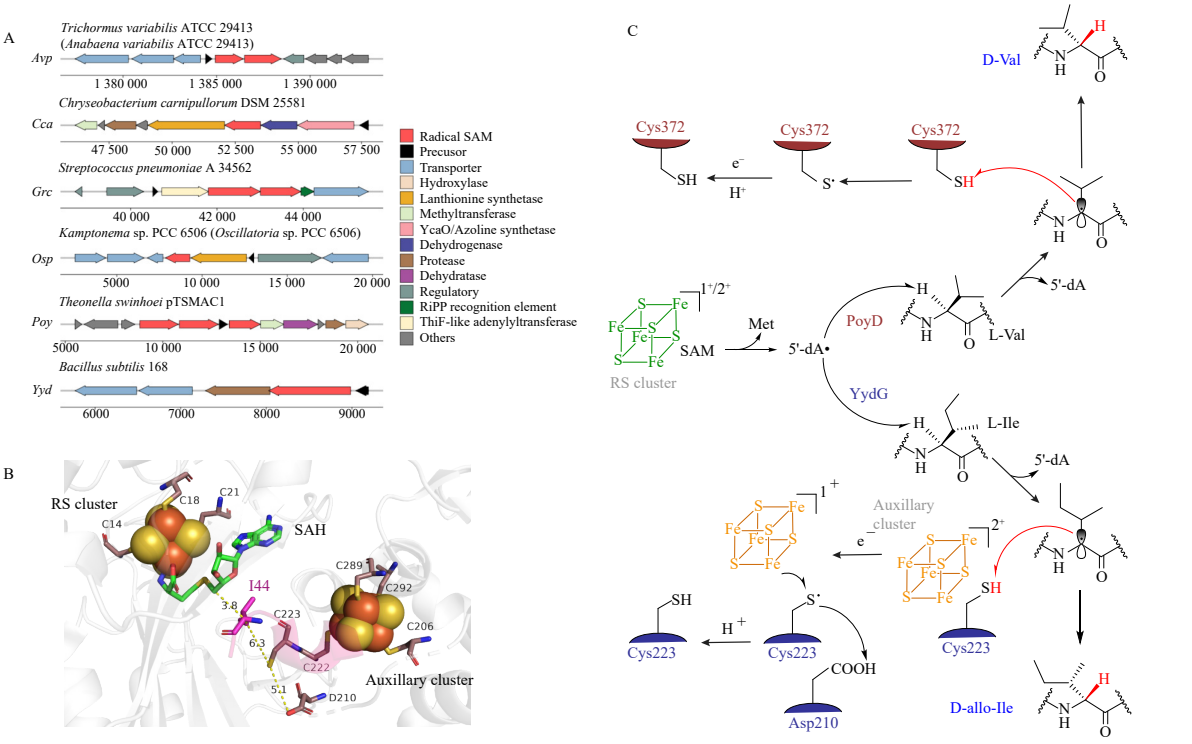

Fig. 3 rSAM-mediated epimerization in RiPPs. (A) The biosynthetic gene clusters of RiPPs containing rSAM that catalyzes epimerization reactions. (B) The proposed catalytic mechanisms of *α*-C epimerization catalyzed by PoyD and YydG. In both cases, the active 5′-dA• generated from SAM cleavage abstracts a hydrogen atom from the substrate. PoyD subsequently provides a hydrogen atom *via* Cys372 for epimerization, while YydG utilizes Cys223 to supply the hydrogen atom, with an additional auxiliary cluster facilitating thiol regeneration. (C) A representative example of rSAM epimerase YydG/EpeE (PDB code: 8AI2). The Ile44 of the precursor peptide is optimally positioned in the active site for catalysis by 5′-dA•, with Cys223 below providing a crucial hydrogen atom to the substrate radical intermediate.

evolved radical-mediated mechanisms to methylate non-nucleophilic substrates, catalyzed by enzymes belonging to the radical SAM superfamily [65].

Zhang et al. [46] initially categorized radical SAM methyltransferases (RSMTs) into three classes based on sequence variations, which have subsequently been expanded to five classes (Fig. 4A) [24, 25, 66, 67]. These RSMTs demonstrate distinct protein structures and catalytic mechanisms. Class A RSMTs, exemplified by RlmN and Cfr, facilitate the methylation of sp^2 carbons of adenine in rRNA, featuring a characteristic rSAM core domain. Class B RSMTs are distinguished by a putative *N*-terminal CBD and a *C*-terminal rSAM domain. These enzymes exhibit a wider substrate range, encompassing inert sp^3 carbons, aromatic heterocycles, and phosphonates. Class C RSMTs display high sequence homology to coproporphyrinogen III oxidase HemN and primarily methylate aromatic heterocycles [68]. Class D RSMTs contain an additional domain that binds to tetrahydrofolate subunits and participate in the methylation of C7 and C9 during methanopterin biosynthesis. Finally, Class E RSMTs, represented by the NifB protein family, catalyze novel carbide insertion reactions during the assembly of nitrogenase metal cofactors.

Class B and Class C RSMTs play a significant role in RiPP biosynthesis. In Class B RSMTs, such as the aforementioned polytheonamide, two B12-dependent rSAM enzymes, PoyB and PoyC, catalyze the methylation of 13 residues at *β*-C and the formation of an unusual *N*-terminal tert-butyl group [69]. PoyC was characterized *in vitro* [70], confirming the production of S-adenosylhomocysteine and 5′-dA, as well as the transfer of a methyl group to L-valine. Isotope labeling experiments utilizing trideuterated SAM (CD_3-SAM) in place of SAM detected a mass increase of approximately 17 Da in the product, establishing SAM as the methyl donor. Additionally, the identification of critical cobalamin cofactors revealed two B12 derivatives in the system: adenosylcobalamin (AdoCbl) and methylcobalamin (MeCbl). Notably, unlike other rSAM enzymes, PoyB and PoyC lack the highly conserved Cx3Cx2C motif, instead possessing a Cx7Cx2C motif, a feature also observed in bottromycin biosynthetic enzymes [71]. In the Ax7Ax2A mutant variant of the rSAM motif, only AdoCbl was observed, indicating the essential role of the iron-sulfur cluster in cobalamin methylation. The Ax7Ax2A mutant variant failed to produce 5′-dA• and SAH, thus losing the capacity to transfer a methyl group to cobalamin to generate MeCbl. In deuterium-labeled experiments with CD_3-SAM, MeCbl was almost completely converted to CD_3-CbI, demonstrating that during catalysis, the enzyme recycles and reutilizes the bound cobalamin from SAM. Regarding the mechanism of methylation transfer to substrates, the authors propose that MeCbl generates a methyl radical intermediate *via* homolytic chemistry, which subsequently bonds with the substrate carbon center radical, similar to methylcoenzyme M reductase chemistry.

TsrM (also known as TsrT) [72, 73] represents another exceptional example of Class B RSMTs. It catalyzes the conversion of tryptophan to 2-methyltryptophan in the *de novo* synthesis of thiostrepton A, a thiopeptide natural product. This conversion ultimately leads to the formation of the quinaldic acid moiety through the action of other modifying enzymes. Despite being an rSAM enzyme, TsrM does not generate the characteristic 5′-dA• typically found in other rSAM enzymes. TsrM can catalyze efficient methylation without sodium dithionite, indicating its independence from external electron donors and confirming the absence of 5′-dA• during the reaction. The coupling of SAH with Me-Trp further demonstrates that SAM functions solely as a methyl donor without radical generation. Cobalamin is essential as a mediator for methyl transfer during the reaction. A labeling experiment (CD_3-SAM) indicates that TsrM utilizes free cob(I)alamin rather than MeCbl directly [72]. Additional research suggests that this process requires a reductant to regenerate MeCbl [74]. Moreover, cobalamins such as adenosylcobalamin or hydroxocobalamin can substitute for methylcobalamin in the system under photochemical or reductive conditions, further demonstrating

the presence of free cobalamin during the reaction. Recently, the crystal structure of TsrM was resolved as the first cobalamin-dependent rSAM methyltransferase (PDB code: 6WTF) [75], elucidating the structural basis for TsrM's free radical-independent catalytic mechanism. TsrM binds a base-off cobalamin, where the axial dimethylbenzimidazole base of the Co ion is uncoordinated (Fig. 4B). Interestingly, the structure reveals that a conserved arginine residue, Arg69, occupies the lower axial position of cobalamin but does not coordinate with Co due to its distance. The charged side chain of Arg69 stabilizes cob(I)alamin as a super nucleophile and destabilizes methylcob(III)alamin, rendering it susceptible to weak nucleophilic attack by the C2 of Trp, supporting the reaction's catalytic mechanism (Fig. 4C). Docking simulations combined with structural insights suggest a dual role for SAM: acting as a methyl donor replaced by cob(I)alamin and its carboxyl group serving as a general base, assisting in deprotonation of N1 of Trp to enhance nucleophilicity at C2. In the docking model, Tyr308 undergoes significant flipping upon substrate binding, potentially acting as a base to facilitate deprotonation at the final C2 position. Furthermore, the structure indicates that the iron-sulfur cluster center of rSAM is coordinated not only by the three cysteine residues in the canonical Cx3Cx2C motif but also by the side-chain carboxylate group of a fully conserved glutamate residue, Glu273, unlike the typical SAM bidentate coordination structure (Fig. 4B). This structural feature explains why TsrM no longer cleaves SAM to produce the 5'-dA• intermediate.

Class C RSMTs include the enzymeNosN [76], which catalyzes the methylation of the indole ring, a reaction mechanistically similar to that of TsrM. However, NosN demonstrates notable differences in substrate specificity and catalytic site configuration. It methylates the C4 position of the indole moiety during nosiheptide maturation [77, 78]. Methylation at the C4 position was confirmed using a thioester derivative substrate formed from N-acetylcysteamine (SNAC) and 3-methylindole-3-acetic acid (MIA). Experiments with CD_3-SAM revealed that the methylated product contains two deuterium atoms, similar to A-class methyltransferases RlmN and Cfr. However, NosN differs in that it does not utilize a cysteine residue as an intermediate methyl group carrier. While significant 5'-dA production occurred during the reaction, minimal SAH was generated. Instead, substantial MTA was produced, suggesting its potential role as an intermediate. Subsequent labeling experiments supported MTA as the direct methyl donor in NosN catalysis, with tAdoH production detected. A proposed catalytic mechanism for NosN was presented (Fig. 4D), wherein one SAM molecule generates MTA, and another produces a 5'-dA • intermediate. Unlike capturing hydrogen atoms from the substrate, the 5'-dA• captures hydrogen from the MTA methyl group, forming a radical intermediate that subsequently reacts with the substrate to form an adduct. Density functional theory (DFT) calculations suggested this adduct likely releases tAdoH *via* a heterolytic pathway, generating the final methylated product. The mechanism of another class C RSMT, TbtI, involved in thiomuracin (a potent thiopeptide antibiotic) methylation, was reported concurrently with NosN. TbtI catalyzes thiazole methylation at the *β*-position. Similar to NosN, TbtI transfers a methylene group from SAM to the substrate rather than a methyl group [79, 80]. One key difference is that TbtI catalyzes the addition between SAM and the substrate, whereas NosN facilitates the addition between 5'-methylthioadenosine and the substrate.

In summary, RSMTs demonstrate diverse catalytic mechanisms and substrate specificities across different enzyme classes. Certain RSMTs, such as TsrM, exhibit broad substrate specificity, catalyzing reactions with various tryptophan derivatives, including melatonin and serotonin (Fig. 4E) [73]. This versatility suggests potential applications for RSMTs in pharmaceutical synthesis and modification processes.

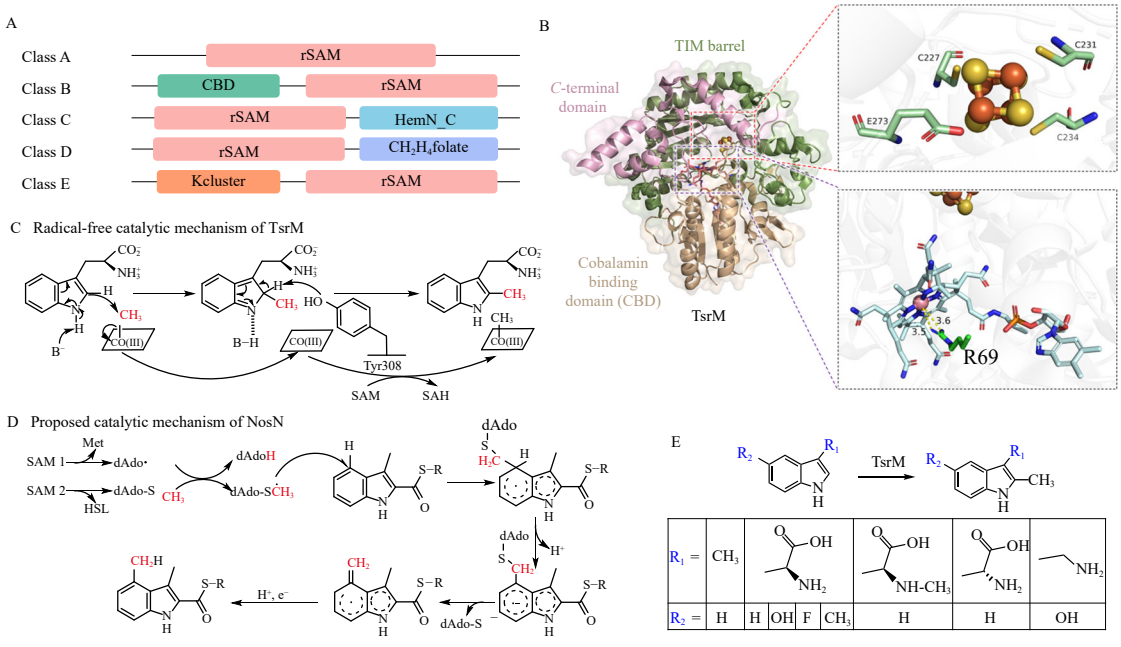

Fig. 4 Different types of rSAM in the methylation of RiPPs. (A) Domain features of five types of RSMTs. In addition to the common rSAM domain, some RSMTs possess auxiliary domains. (B) TsrM (PDB code: 6WTF), a representative class B rSAM methyltransferase. It comprises an *N*-terminal CBD, the characteristic partial TIM barrel domain of rSAM, and a *C*-terminal extension. The inset illustrates the unique, fully coordinated core iron-sulfur cluster and the key residue Arg69, which facilitates in the coordination of the cobalamin cofactor. (C) A proposed catalytic mechanism for TsrM that is not dependent on radicals. MeCbl obtains a methyl group from SAM, serving as a methyl intermediate carrier. The substrate Trp receives the methyl group from MeCbl *via* an SN2 nucleophilic substitution, potentially followed by Tyr308-assisted deprotonation. Cobalamin then regenerates to MeCbl by obtaining a new methyl group from SAM. (D) Proposed catalytic mechanism of NosN. Two SAM molecules generate 5'-dA• and 5'-methylthioadenosine (MTA), respectively. The 5'-dA• abstracts a hydrogen atom from MTA's methylthio group, forming an MTA radical that attacks the substrate at the C4 position, creating an adduct. Subsequently, C4 position deprotonation occurs, accompanied by 5'-thioadenosine (tAdoH) heterolysis. With an additional proton and electron, the final product forms. (E) Substrate promiscuity catalyzed by TsrM. Beyond the natural substrate Trp, TsrM exhibits methylation activity on substrates with C3 and C5 indole ring substitutions, including melatonin and serotonin.

4. Thioether formation

Thioether bond-containing peptide natural products, such as the extensively studied lanthipeptides [81], feature a characteristic *β*-thioether bond formed between Cys and Ser/Thr side chains, known as lanthionine. Multi-domain proteins catalyze lanthionine formation through a series of steps, including phosphorylation activation, elimination reactions, and Michael addition cyclization. In contrast, rSAM enzymes employ a radical mechanism to catalyze a one-step reaction, forming a thioether bond connecting Cα, Cβ, and Cγ. This process extends the range of recipient residues beyond Ser and Thr to encompass 20 other common amino acids, thus expanding the chemical diversity of sulfur-containing peptide natural products [41, 42, 82].

The rSAM-catalyzed S-Cα-linked thioether reaction of peptides was initially observed in the biosynthesis of subtilosin A, a 20-residue tetracyclic peptide [83]. Subsequently, researchers have identified other natural peptides containing S-Cα linkages, including thurincin H [83, 84], thuricin CD (comprising two peptides Trn-α and Trn-β) [85, 86], sporulation killing factor [87, 88], hyicin 4244 [89], thuricin Z/huazacin [82, 90], ruminococcin C [91-93], and streptosactin [94] (Fig. 5A). These peptides, which form Cα-S thioether bonds catalyzed by rSAM enzymes, are termed sactipeptides (sulfur-to-alpha carbon thioether cross-linked peptides), and the rSAM enzymes catalyzing these unique thioether bonds are referred to as sactisynthases [41, 42]. Most sactipeptides exhibit antimicrobial activity, with some also demonstrating spermicidal and hemolytic activities [42, 95]. Structurally, sactipeptides typically feature multiple Cys residues at the *N*-terminus, while the receptor residues forming thioether pairs are located at the *C*-terminus. These structural characteristics dictate their specific conformations, with sactipeptides often adopting nested hairpin structures around the thioether bond. Notable exceptions include the dual hairpin structure found in ruminococcin C [93], and streptosactin [94], which adopts consecutive double-ring structures rather than a hairpin conformation.

The rSAM enzymes catalyzing inter-side chain Cα-S thioether cross-links, also known as sactisynthases, typically comprise a partial TIM barrel domain similar to other rSAM enzymes. Additionally, they often possess a *C*-terminal SPASM/Twitch domain for binding additional auxiliary iron-sulfur clusters, and an *N*-terminal RRE domain involved in precursor peptide recognition. For instance, studies of the rSAM enzyme AlbA in subtilosin A biosynthesis [95] demonstrated through mutation experiments that the absence of the auxiliary cluster did not affect the rSAM enzyme's activity in cleaving SAM, but it no longer produced thioether cross-links. This suggests that the auxiliary cluster plays a crucial role in the catalytic reaction. Furthermore, changes in UV-visible absorption bands indicate direct interactions between the auxiliary cluster and the precursor peptide.

Based on these findings, a mechanistic model has been proposed wherein the auxiliary cluster binds to the active Cys residue in the substrate (Fig. 5B). The reaction initiates with the reductive cleavage of SAM, generating a 5'-dA• that abstracts a hydrogen from the *α*-carbon atom of the receptor residue, forming a substrate radical intermediate. Concurrently, the thiol of the active Cys in the substrate undergoes deprotonation and coordinates with the auxiliary cluster. Subsequently, the substrate radical intermediate attacks the Fe-S bond, inducing homolytic cleavage, accompanied by electron transfer to the auxiliary cluster. Ultimately, the redox valence states of the core and auxiliary clusters are reset through internal electron transfer or *via* an external redox system, enabling the next catalytic cycle.

Furthermore, a ketoimine mechanism has been proposed [96, 97]. In this mechanism, the 5'-dA• resulting from SAM cleavage initially abstracts the *α*-H of the receptor residue, generating an *α*-carbon radical intermediate. This intermediate subsequently undergoes electron transfer to form a reactive imine intermediate, which then reacts with the nucleophilic cysteine thiol group to produce a thioether. Notably, the auxiliary cluster facilitates the electron transfer in this process.

It is significant to note that in the rSAM-catalyzed thioether cross-linking of peptide side chains, certain instances involve the receptor residues undergoing stereochemical transformation from L- to D-configuration [93, 98]. The stereochemical outcome may be related to the spatial arrangement of the substrates, analogous to the biosynthesis of lanthipeptides, which involves the structural rearrangement of *α*-carbon radical intermediates [98]. For instance, subtilosin A adopts an LDD configuration, thurincin H displays a DDDD configuration, and ruminococcin C maintains an LLLL configuration. The catalytic mechanisms governing these configurational differences remain unclear, necessitating further investigation to identify and characterize key catalytic intermediates involved in these processes.

In addition to Cα-S cross-links, the rSAM enzyme can also introduce thioether bonds at the Cβ and Cγ positions [82, 99, 100] (Fig. 5C). Thermocellin, containing a single thioether bond, was initially classified within the sactipeptides subfamily [99]. The Cα-S thioether cross-link between Cys and Thr in its precursor peptide CteA is catalyzed by the rSAM enzyme CteB. Subsequently, Hudson and colleagues [82] utilized isotope labeling experiments to demonstrate that this thioether bond is positioned at the γ carbon of Thr, forming a Cγ-S thioether. Notably, this acceptor Thr is only one residue away from the donor Cys, in contrast to the previously reported four residues away from the Thr. Furthermore, Hudson et al. [82] employed bioinformatics tools to identify freyrasin, which contains six Cβ-S thioether bonds between Cys and Asp. *In vitro* experiments confirmed that the synthesis of these six thioether bonds in the precursor peptide PapA is catalyzed by the rSAM enzyme PapB. The resulting product exhibits a novel topology distinct from the hairpin structure of sactipeptides. Consequently, Hudson et al. redefined peptides like freyrasin and thermocellin, which contain Cβ and Cγ thioether cross-links, as a new class of sulfur-containing peptides called ranthipeptides (radical non-α thioether peptides). Additionally, Caruso and colleagues [100] identified the rSAM enzyme NxxcB in streptococci catalyzing a Cβ-S thioether bond between Asn and Cys, leading to a new class of rathipeptide containing a single Cβ-S thioether bond.

5. Side-chain C-C/heteroatom cross-links

Cyclic peptides in peptide therapeutics offer notable advantages over their linear counterparts, including enhanced resistance to enzymatic degradation and improved receptor binding due to their rigid ring structures [101]. While traditional cyclization occurs *via* amide bonds between peptide termini, there is increasing interest in products cyclized through side-chain to side-chain interactions, typically forming cross-link structures *via* C-C/heteroatom bonds [26, 43, 102-106]. Examples include sulfur bridges formed by dehydration cyclization of lanthipeptides [81], catalyzed by multi-domain proteins; aromatic C-C and C-O couplings catalyzed by P450 enzymes in Cittilin [107]; aromatic C-C cross-links in biarylitides [108]; and aromatic couplings during assembly of non-ribosomal peptides such as vancomycin and kistamicin [109]. Furthermore, an emerging class of C-C/heteroatom side-chain cross-linking reactions catalyzed by rSAM enzymes is gaining prominence in recent discoveries.

5.1. Side-chain C-C cross-linking

Streptide [26, 104, 105] exemplifies side-chain C-C cross-linking in ribosomally synthesized and post-translationally modified peptides facilitated by rSAM enzymes. Produced by the pathogenic

thermophilic bacterium *Streptococcus thermophilus*, streptide forms a distinctive C-C cross-link between the inert *β*-carbon of lysine (Lys) and the indole C7 of tryptophan, a reaction catalyzed by the metalloenzyme StrB [26]. StrB comprises a typical rSAM core domain and incorporates a SPASM domain at its *C*-terminus, indicating potential interaction with an auxiliary iron-sulfur cluster. Substrate experiments confirm that StrB catalyzes leader-dependent reactions. Notably, the mutation of cysteine residues coordinating the auxiliary iron-sulfur cluster to alanine eliminates catalytic activity, underscoring the auxiliary cluster's crucial role in the catalytic process.

SuiB [104], encoded by *Streptococcus suis*, exhibits 96% homology with StrB and similarly catalyzes the C-C cross-linking reaction between Lys and Trp. X-ray crystallography and computational simulations have elucidated the binding mechanism of SuiB with its substrate SuiA. SuiB comprises three functional domains: an *N*-terminal RRE domain (1–106), an rSAM domain (107–310), a short bridging domain (311–346), and a *C*-terminal SPASM domain (347–437) (Fig. 6A). The SPASM domain contains a characteristic 7-Cys motif ($Cx_{9-15}Gx_4C$–gap–$Cx_2Cx_5Cx_3C$–gap–C), which binds two additional auxiliary iron-sulfur clusters and forms a closure with the TIM barrel of the core domain, thus creating a catalytic cavity. The RRE domain is involved in precursor peptide recognition, ensuring proper substrate positioning for catalysis through interactions with the leader peptide. However, interactions between the RRE structural domains of SuiA and SuiB are limited; instead, unique hydrogen bonding interactions between the highly conserved LESS motifs in the precursor sequences and the bridging region predominantly govern SuiA recognition in the active site. These interactions orient the substrate helix, facilitating proper alignment of the core sequence in the active site (Fig. 6A).

A comparison of the substrate-free and SAM-bound crystal structures reveals that loops L1 (residues 125–134) and L2 (residues 279–285) adopt a new conformation in the SuiA-bound structure, effectively closing the active site and impeding solvent entry. This restriction of solvent entry by L2 induces a dielectric change in the active site, which has been previously hypothesized to contribute to lowering the free energy barrier for SAM cleavage. Additionally, associated channels connect AuxI with SuiA, suggesting that loop movements may play a critical role in redox reactions involving AuxI. Rosetta-based simulations further elucidate how the leader sequence facilitates proper substrate positioning. Moreover, Glu319 was identified as the closest residue to the C7 residue of SuiA-W6 (within approximately 5 Å), potentially serving as a general base pair reaction intermediate for deprotonation.

Two mechanisms were proposed for the Lys-Trp side-chain cross-linking in streptide: one involving typical electrophilic aromatic substitution (EAS) and another involving radical electrophilic aromatic substitution (rEAS). Recent research by Aidin et al. [105] provided direct evidence supporting the rEAS mechanism. Through electron paramagnetic resonance (EPR) spectroscopy and DFT calculations, they identified a critical radical intermediate, lysine-tryptophan radical (Lys-Trp •). This intermediate forms a radical-σ complex *via* an alkyl radical attack on the tryptophan indole ring. Furthermore, substrate binding regulates the redox states of the RS and auxiliary I (Aux I) clusters. Upon substrate binding, the RS cluster undergoes reduction, preparing it for SAM reaction, while the Aux I cluster is oxidized, potentially functioning as a low-potential oxidant for the radical intermediate.

Based on the collective evidence, a comprehensive catalytic mechanism for SuiB is proposed (Fig. 6B). The process initiates with substrate binding, which recalibrates the redox states of the rSAM and Aux I clusters. Subsequently, an electron transfer from the RS cluster facilitates the reductive cleavage of SAM, resulting in the release of a 5'-dA•. This radical then abstracts a hydrogen atom from the *β*-position of Lys, generating an alkyl radical intermediate. The alkyl radical intermediate proceeds to attack the tryptophan indole ring, forming a Lys-Trp•. The final product is hypothesized to form through Glu319-assisted deprotonation, followed by an Aux I-mediated oxidation.

In addition to SuiB, the rEAS pathway may serve as a foundation for other rSAM enzymes that catalyze similar sp^2-sp^3 carbon-carbon cross-links. For example, a subclass of RiPPs called ryptides [103] (R-Y-cross-linked peptides) is found in *Streptococcus suis*. The corresponding *rrr* biosynthetic gene cluster (*rrr* BGC) encodes the precursor (RrrA), an rSAM enzyme (RrrB), and a transporter protein (RrrC). *In vivo* characterization studies of

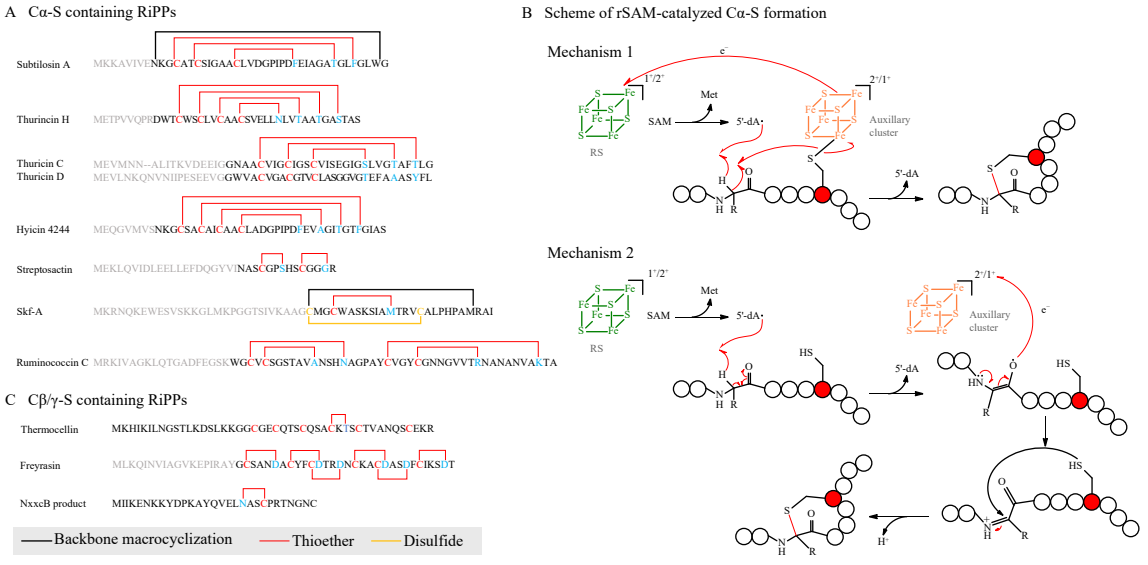

Fig. 5 rSAM-mediated formation of S-Cα, S-Cβ, and S-Cγ thioether in RiPPs. (A) Representative examples of Sactipeptides containing Cα-S thioether bonds. (B) Proposed rSAM-catalyzed Cα-S thioether formation mechanisms. In mechanism 1, the reactive 5'-dA• abstracts a hydrogen atom from the Cα of the acceptor residue concurrent with the formation of an adduct between the donor Cys and the auxiliary iron-sulfur cluster. Subsequently, the acceptor residue radical intermediate attacks the Fe-S bond, forming a thioether bond and transferring an electron to the auxiliary cluster. Electron transfer between the auxiliary cluster and the RS core cluster restores the redox state of the iron-sulfur cluster. In mechanism 2, the substrate, following hydrogen atom abstraction by 5'-dA•, forms an imine intermediate, which is then attacked by Cys-SH to produce a thioether. (C) Natural products of the Ranthipeptide class containing Cβ/γ-S thioether bonds.

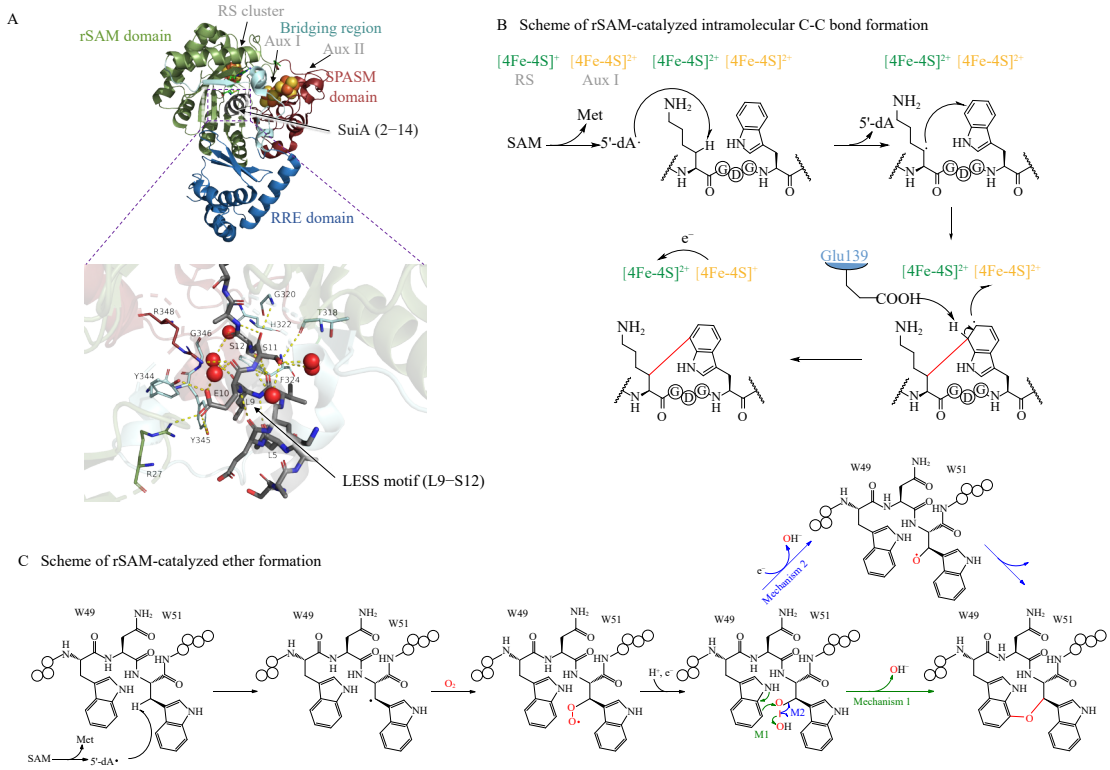

Fig. 6 rSAM-mediated formation of C-C and C-X bonds in RiPPs. (A) Example of an rSAM enzyme that catalyzes C-C cross-linking between peptide chain side chains: SuiB (PDB ID: 5V1T). In addition to the typical rSAM structural domain, additional *C*-terminal RRE structural domains and *N*-terminal SPASM structural domains are present, with a bridging region connecting the rSAM structural domain to the SPASM structural domain. The box illustrates the hydrogen bonding interaction network between the conserved LESS motif of the precursor peptide and the residues in the active cavity. (B) Proposed catalytic mechanism of SuiB. 5'-dA• generated by SAM cleavage abstracts a hydrogen atom at the *β*-position of Lys, followed by the radical intermediate attacking the C7-position of the Trp indole ring to form a Lys-Trp• intermediate. Subsequently, Glu319 may function as a general base to assist in deprotonation of the Lys-Trp• intermediate to produce the end product. The auxiliary and core clusters reset the redox potential through internal or external electron transfer to proceed to the next catalytic cycle. (C) Proposed mechanism for ether cross-link formation catalyzed by DarE. The 5'-dA• generated from SAM cleavage abstracts a hydrogen atom at the *β*-position of W51, forming a radical intermediate. Subsequently, addition to O_2 is accompanied by proton and electron transfer to produce a hydroperoxide intermediate. Ultimately, ether bonds are generated *via* heterolytic or homolytic chemistry.

RrrB have shown that its catalytic C-C cross-linking occurs at the *δ*-carbon of Arg adjacent to the phenolic hydroxyl group of Tyr. Notably, the catalytic activity of RrrB does not require the presence of the leader peptide.

Kenzie and Mohammad [102] utilized bioinformatics techniques to analyze and cluster rSAM enzymes containing SPASM/Twich domains from extensive databases. Employing co-occurrence and co-conservation principles between precursor peptides and modifying enzymes, along with developed precursor prediction algorithms, they categorized approximately 15 500 uncharacterized biosynthetic gene clusters into 800 subfamilies. This comprehensive effort resulted in a bioinformatics atlas of rSAM-modified RiPP natural products. Investigation of the ITF subfamily, exemplified by the *itf* gene cluster from *Bacteroides thetaiotaomicron*, revealed a cross-linking reaction catalyzed by the rSAM enzyme ItfD between the C7 of Trp and the *δ*-carbon of Ile. This finding confirms the viability of this method for discovering novel rSAM enzymes that catalyze the formation of unique chemical scaffolds, thus expanding the chemical space of rSAM enzyme-mediated C-C cross-linking reactions.

5.2. Side-chain C-O cross-linking

rSAM enzymes facilitate an additional category of side-chain cross-linking reactions involving C-heteroatom bonds. A notable example is darobactin [4], a ribosomally synthesized and post-translationally modified peptide renowned for its potent activity against Gram-negative bacteria. In its structure, alongside the previously mentioned C-C cross-link between W3 and K5, there exists a C-O cross-link between W1 and W3.

The C-C/O cross-links in Darobactin [110, 111] are confirmed to be catalyzed by a single rSAM enzyme, DarE [43], which also contains a *C*-terminal SPASM/Twitch domain coordinating additional auxiliary iron-sulfur clusters. *In vitro* characterization of DarE indicates that the C-O cross-linking precedes the C-C cross-linking, potentially representing the initial modification step in darobactin biosynthesis. Initial experiments utilizing $H_2{}^{18}O$ as a solvent for the reaction resulted in an ^{18}O-containing product, suggesting that the oxygen atom in the ether bond of darobactin originates from H_2O. However, subsequent research by Nguyen et al. demonstrated that O_2 is the oxygen donor to this reaction using $^{18}O_2$ [112]. Further analysis by MS/MS revealed that the mass shift from ^{18}O incorporation from $H_2{}^{18}O$ was added to other residues rather than the ether bond, an artifact of protease treatment [113]. Based on these findings, a DarE-catalyzed reaction mechanism was proposed. In this mechanism, 5'-dA• from SAM cleavage abstracts hydrogen at the W51 *β*-position, generating a radical intermediate. Subsequently, O_2 doping, accompanied by proton and electron migration, produces a hydroperoxide intermediate. The reaction can then form ether bonds through either heterolytic or homolytic chemistry. In the first proposed mechanism, the indole ring of W49 nucleophilically attacks the hydroperoxide intermediate, followed by re-aromatization. Alternatively, in the second mechanism, the hydroperoxide undergoes homolytic cleavage, generating an alkoxy radical that attacks the indole ring of W49. This process, accompanied by the loss of a proton and an electron, forms an ether bond between the side chains of W49 and W51.

Kenzie et al. [106] identified the first rSAM enzyme-catalyzed *α*-ether bond reaction between side chains of RiPPs, designating these peptides as rotapeptides (radical oxygen-to-alpha carbon-linked peptides). The rSAM enzyme TqqB, which catalyzes this C-O cross-link, incorporates a Twitch domain to coordinate an auxiliary cluster. Mechanistic studies of TqqB suggest it may em-

ploy a mechanism akin to the formation of thioether bonds catalyzed by rSAM enzymes. In this process, the auxiliary cluster interacts with oxygen atoms from the substrate, followed by hydrogen atom abstraction by the 5'-dA• at the α-carbon, attacking the Fe-O bond to generate the final product, accompanied by electron transfer to the auxiliary cluster. The transfer of electrons between the auxiliary and RS clusters may occur through internal electron transfer or mediation by an external redox partner, resetting the oxidation state of the iron-sulfur clusters to initiate the next catalytic cycle.

5.3. Side-chain C-N and other cross-linking

rSAM enzymes catalyzing side-chain C-N linkages [114] are increasingly being discovered. Leah and colleagues identified a novel class of side-chain bicyclic peptides, termed bicyclostreptins, from *Streptococcus* sp. The bicyclic structure of these peptides is formed by a β-thioether bond and the sp^3-sp^3 N-C cross-linking of the backbone amide N and the adjacent α-C, respectively. Two rSAM enzymes, HghB and HghC, catalyze these two side-chain rings sequentially. This research also demonstrates that bicyclostreptins function as potent growth regulators in Thermophilic *Streptococcus*. Furthermore, other types of C-C/heteroatom cross-linking reactions in RiPPs natural products are being elucidated with increasing frequency, involving a diverse array of substrate residues and sites [115-118].

6. Others

rSAM enzymes are known for their versatile catalytic capabilities, particularly in facilitating oxidation reactions. In the biosynthesis of mycofactocin [29], the bifunctional rSAM enzyme MftC initially catalyzes the oxidative decarboxylation of the *C*-terminal Tyr residue in the precursor peptide MftA. This process results in the elimination of a carboxyl group and the formation of a new α/β-unsaturated bond. Subsequently, MftC proceeds to catalyze the sp^3-sp^2 C-C cross-linking reaction between the adjacent Val and Tyr residues. In *Streptococcus pneumoniae* A 34562 [44], researchers identified a biosynthetic gene cluster *grc*-encoding RiPPs. Within this cluster, two rSAM enzymes, GrcC and GrcD, catalyze the β-epimerization of L-Thr and the α,β-dehydrogenation of L-His in the precursor peptide GrcA, respectively.

Furthermore, rSAM enzymes have exhibited the ability to catalyze complex rearrangement reactions. For instance, the 3-methylindole acid moiety in the nosiheptide structure is derived from L-Trp through a rearrangement reaction catalyzed by the rSAM enzyme NosL [45]. In addition to the six types of reactions previously described, rSAM enzymes catalyze various other reactions in the biosynthesis of natural products that have yet to be reported in RiPPs [119]. The potential roles of these enzymes in expanding the diversity of RiPPs warrant further investigation.

7. Conclusions and outlook

This work summarizes the crucial roles of currently known rSAM enzymes in the post-translational modification of RiPPs, including Cα and Cβ epimerization, side-chain methylation, S-Cα-γ thioether, unusual C-C/heteroatom cross-linking, oxidation, and rearrangement. The structural features of representative rSAMs and their associated catalytic mechanisms are thoroughly examined, potentially informing the development of biomimetic chemistry with high specificity and selectivity. Recent advancements in sequencing technology have led to a significant increase in data volume and the creation of new tools for gene mining. Systematic exploration using bioinformatics tools has yielded promising results in the discovery of potential RiPPs and novel rSAM enzymes. For example, mining homologous rSAM enzymes that catalyze ether bond formation from known DarEs has resulted in the practical discovery of new daropeptides and expanded the catalytic range of such enzymes. Recent studies of rSAMs have also demonstrated wide substrate adaptabilities, indicating their potential as broad-spectrum biocatalysts for chemical modification. As more rSAMs are discovered and characterized, the diversity of uncovered catalytic mechanisms continues to expand. With the support of structural resolution techniques, an improved understanding of the enzymes' functional domains and their interactions, as well as an in-depth analysis of enzyme-substrate complexes, facilitates the elucidation of catalytic mechanisms for this large class of enzymes. The growing diversity of rSAM enzymes, deeper understanding of catalytic mechanisms, and mechanism-based engineering of rSAM enzymes are expected to significantly advance research in synthesizing high-value active natural products and derivatives.

Funding

This work was supported by the National Key Research and Development Program of China (No. 2023YFA0916000), the National Natural Science Foundation of China (No. 32371324), and the High-level Talent Startup Fund provided by China Pharmaceutical University.

Declaration of competing interest

These authors have no conflict of interest to declare.

References

1 Montalbán-López M, Scott TA, Ramesh S, et al. New developments in RiPP discovery, enzymology and engineering. *Nat Prod Rep*. 2021;38(1):130-239. https://doi.org/10.1039/D0NP00027B.
2 Peng H, Wang J, Chen J, et al. Challenges and opportunities in delivering oral peptides and proteins. *Expert Opin Drug Deliv*. 2023;20(10):1349-1369. https://doi.org/10.1080/17425247.2023.2237408.
3 Lubelski J, Rink R, Khusainov R, et al. Biosynthesis, immunity, regulation, mode of action and engineering of the model lantibiotic nisin. *Cell Mol Life Sci*. 2008;65(3):455-476. https://doi.org/10.1007/s00018-007-7171-2.
4 Imai Y, Meyer KJ, Iinishi A, et al. A new antibiotic selectively kills Gram-negative pathogens. *Nature*. 2019;576(7787):459-464. https://doi.org/10.1038/s41586-019-1791-1.
5 Ding W, Liu WQ, Jia Y, et al. Biosynthetic investigation of phomopsins reveals a widespread pathway for ribosomal natural products in Ascomycetes. *Proc Natl Acad Sci U S A*. 2016;113(13):3521-3526. https://doi.org/10.1073/pnas.1522907113.
6 Wang L, Li MD, Cao PP, et al. Astin B, a tide from *Aster tataricus*, induces apoptosis and autophagy in human hepatic L-02 cells. *Chem Biol Interact*. 2014;223:1-9. https://doi.org/10.1016/j.cbi.2014.09.003.
7 Akondi KB, Muttenthaler M, Dutertre S, et al. Discovery, synthesis, and structure-activity relationships of conotoxins. *Chem Rev*. 2014;114(11):5815-5847. https://doi.org/10.1021/cr400401e.
8 Kong Y, Wang Y, Yang W, et al. LX0702, a novel snake venom peptide derivative, inhibits thrombus formation *via* affecting the binding of fibrinogen with GPIIb/IIIa. *J Pharmacol Sci*. 2015;127(4):462-466. https://doi.org/10.1016/j.jphs.2015.03.010.
9 Zou X, He Y, Qiao J, et al. The natural scorpion peptide, BmK NT1 activates voltage-gated sodium channels and produces neurotoxicity in primary cultured cerebellar granule cells. *Toxicon*. 2016;109:33-41. https://doi.org/10.1016/j.toxicon.2015.11.005.
10 Yang HL, Shen ZQ, Liu X, et al. Two novel antimicrobial peptides from skin venoms of spadefoot toad *Megophrys minor*. *Chin J Nat Med*. 2016;14(4):294-298. https://doi.org/10.1016/S1875-5364(16)30030-9.
11 Jin AH, Muttenthaler M, Dutertre S, et al. Conotoxins: chemistry and biology. *Chem Rev*. 2019;119(21):11510-11549. https://doi.org/10.1021/acs.chemrev.9b00207.
12 Zou X, Wang Y, Yu Y, et al. BmK NSP, a new sodium channel activator from *Buthus martensii* Karsch, promotes neurite outgrowth in primary cultured spinal cord neurons. *Toxicon*. 2020;182:13-20. https://doi.org/10.1016/j.toxicon.2020.04.096.
13 Zheng YZ, Ji XR, Liu YY, et al. WPK5, a novel kunitz-type peptide from the leech *Whitmania pigra* inhibiting factor XIa, and its loop-replaced mutant to improve potency. *Biomedicines*. 2021;9(12):1745. https://doi.org/10.3390/biomedicines9121745.
14 Jia Z, Liu Y, Ji X, et al. DAKS1, a kunitz scaffold peptide from the venom gland of *Deinagkistrodon acutus* prevents carotid-artery and middle-cerebral-artery thrombosis *via* targeting factor XIa. *Pharmaceuticals*. 2021;14(10):966. https://doi.org/10.3390/ph14100966.
15 Huang J, Song W, Hua H, et al. Antithrombotic and anticoagulant effects of a novel protein isolated from the venom of the *Deinagkistrodon acutus* snake. *Biomed Pharmacother*. 2021;138:111527. https://doi.org/10.1016/j.biopha.2021.111527.
16 Li T, Xi C, Yu Y, et al. Targeted discovery of amantamide B, an ion channel

modulating nonapeptide from a South China Sea *Oscillatoria* cyanobacterium. *J Nat Prod*. 2022;85(3):493-500. https://doi.org/10.1021/acs.jnatprod.1c00983.
17 Colgrave ML, Kotze AC, Kopp S, et al. Anthelmintic activity of cyclotides: *in vitro* studies with canine and human hookworms. *Acta Trop*. 2009;109(2):163-166. https://doi.org/10.1016/j.actatropica.2008.11.003.
18 Morita H, Shimbo K, Shigemori H, et al. Antimitotic activity of moroidin, a bicyclic peptide from the seeds of *Celosia argentea*. *Bioorg Med Chem Lett*. 2000;10(5):469-471. https://doi.org/10.1016/s0960-894x(00)00029-9.
19 Liu FJ, Zhu ZH, Jiang Y, et al. A pair of cyclopeptide epimers from the seeds of *Celosia argentea*. *Chin J Nat Med*. 2018;16(1):63-69. https://doi.org/10.1016/S1875-5364(18)30030-X.
20 Kersten RD, Mydy LS, Fallon TR, et al. Gene-guided discovery and ribosomal biosynthesis of moroidin peptides. *J Am Chem Soc*. 2022;144(17):7686-7692. https://doi.org/10.1021/jacs.2c00014.
21 Hetrick KJ, Van Der DWA. Ribosomally synthesized and post-translationally modified peptide natural product discovery in the genomic era. *Curr Opin Chem Biol*. 2017;38:36-44. https://doi.org/10.1016/j.cbpa.2017.02.005.
22 Funk MA, Van Der DWA. Ribosomal natural products, tailored to fit. *Acc Chem Res*. 2017;50(7):1577-1586. https://doi.org/10.1021/acs.accounts.7b00175.
23 Freeman MF, Gurgui C, Helf MJ, et al. Metagenome mining reveals polytheonamides as posttranslationally modified ribosomal peptides. *Science*. 2012;338(6105):387-390. https://doi.org/10.1126/science.1226121.
24 Fujimori DG. Radical SAM-mediated methylation reactions. *Curr Opin Chem Biol*. 2013;17(4):597-604. https://doi.org/10.1016/j.cbpa.2013.05.032.
25 Bauerle MR, Schwalm EL, Booker SJ. Mechanistic diversity of radical S-adenosylmethionine (SAM)-dependent methylation. *J Biol Chem*. 2015;290(7):3995-4002. https://doi.org/10.1074/jbc.R114.607044.
26 Schramma KR, Bushin LB, Seyedsayamdost MR. Structure and biosynthesis of a macrocyclic peptide containing an unprecedented lysine-to-tryptophan crosslink. *Nat Chem*. 2015;7(5):431-437. https://doi.org/10.1038/nchem.2237.
27 Parent A, Benjdia A, Guillot A, et al. Mechanistic investigations of PoyD, a radical S-adenosyl-L-methionine enzyme catalyzing iterative and directional epimerizations in polytheonamide A biosynthesis. *J Am Chem Soc*. 2018;140(7):2469-2477. https://doi.org/10.1021/jacs.7b08402.
28 Morinaka BI, Lakis E, Verest M, et al. Natural noncanonical protein splicing yields products with diverse *β*-amino acid residues. *Science*. 2018;359(6377):779-782. https://doi.org/10.1126/science.aao0157.
29 Ayikpoe R, Govindarajan V, Latham JA. Occurrence, function, and biosynthesis of mycofactocin. *Appl Microbiol Biotechnol*. 2019;103(7):2903-2912. https://doi.org/10.1007/s00253-019-09684-4.
30 Sofia HJ, Chen G, Hetzler BG, et al. Radical SAM, a novel protein superfamily linking unresolved steps in familiar biosynthetic pathways with radical mechanisms: functional characterization using new analysis and information visualization methods. *Nucleic Acids Res*. 2001;29(5):1097-1106. https://doi.org/10.1093/nar/29.5.1097.
31 Frey PA, Hegeman AD, Ruzicka FJ. The radical SAM superfamily. *Crit Rev Biochem Mol Biol*. 2008;43(1):63-88. https://doi.org/10.1080/10409230701829169.
32 Vey JL, Drennan CL. Structural insights into radical generation by the radical SAM superfamily. *Chem Rev*. 2011;111(4):2487-2506. https://doi.org/10.1021/cr9002616.
33 Benjdia A, Balty C, Berteau O. Radical SAM enzymes in the biosynthesis of ribosomally synthesized and post-translationally modified peptides (RiPPs). *Front Chem*. 2017;5:87. https://doi.org/10.3389/fchem.2017.00087.
34 Mahanta N, Hudson GA, Mitchell DA. Radical S-adenosylmethionine enzymes involved in RiPP biosynthesis. *Biochemistry*. 2017;56(40):5229-5244. https://doi.org/10.1021/acs.biochem.7b00771.
35 Benjdia A, Berteau O. Radical SAM enzymes and ribosomally-synthesized and post-translationally modified peptides: a growing importance in the microbiomes. *Front Chem*. 2021;9:678068. https://doi.org/10.3389/fchem.2021.678068.
36 Moody JD, Hill S, Lundahl MN, et al. Computational engineering of previously crystallized pyruvate formate-lyase activating enzyme reveals insights into SAM binding and reductive cleavage. *J Biol Chem*. 2023;299(6):104791. https://doi.org/10.1016/j.jbc.2023.104791.
37 Broderick JB, Duffus BR, Duschene KS, et al. Radical S-adenosylmethionine enzymes. *Chem Rev*. 2014;114(8):4229-4317. https://doi.org/10.1021/cr4004709.
38 Horitani M, Shisler K, Broderick WE, et al. Radical SAM catalysis *via* an organometallic intermediate with an Fe-[5′-C]-deoxyadenosyl bond. *Science*. 2016;352(6287):822-825. https://doi.org/10.1126/science.aaf5327.
39 Hoffman BM, Broderick WE, Broderick JB. Mechanism of radical initiation in the radical SAM enzyme superfamily. *Annu Rev Biochem*. 2023;92:333-349. https://doi.org/10.1146/annurev-biochem-052621-090638.
40 Ogasawara Y, Dairi T. Peptide epimerization machineries found in microorganisms. *Front Microbiol*. 2018;9:156. https://doi.org/10.3389/fmicb.2018.00156.
41 Flühe L, Marahiel MA. Radical S-adenosylmethionine enzyme catalyzed thioether bond formation in sactipeptide biosynthesis. *Curr Opin Chem Biol*. 2013;17(4):605-612. https://doi.org/10.1016/j.cbpa.2013.06.031.
42 Chen Y, Wang J, Li G, et al. Current advancements in sactipeptide natural products. *Front Chem*. 2021;9:595991. https://doi.org/10.3389/fchem.2021.595991.
43 Guo S, Wang S, Ma S, et al. Radical SAM-dependent ether crosslink in daropeptide biosynthesis. *Nat Commun*. 2022;13(1):2361. https://doi.org/10.1038/s41467-022-30084-2.
44 Johnson BA, Clark KA, Bushin LB, et al. Expanding the landscape of noncanonical amino acids in RiPP biosynthesis. *J Am Chem Soc*. 2024;146(6):3805-3815. https://doi.org/10.1021/jacs.3c10824.
45 Zhang Q, Li Y, Chen D, et al. Radical-mediated enzymatic carbon chain fragmentation-recombination. *Nat Chem Biol*. 2011;7(3):154-160. https://doi.org/10.1038/nchembio.512.
46 Zhang Q, Van Der DWA, Liu W. Radical-mediated enzymatic methylation: a tale of two SAMS. *Acc Chem Res*. 2012;45(4):555-564. https://doi.org/10.1021/ar200202c.
47 Grell TAJ, Goldman PJ, Drennan CL. SPASM and twitch domains in S-adenosylmethionine (SAM) radical enzymes. *J Biol Chem*. 2015;290(7):3964-3971. https://doi.org/10.1074/jbc.R114.581249.
48 Bushin LB, Clark KA, Pelczer I, et al. Charting an unexplored streptococcal biosynthetic landscape reveals a unique peptide cyclization motif. *J Am Chem Soc*. 2018;140(50):17674-17684. https://doi.org/10.1021/jacs.8b10266.
49 He B, Cheng Z, Zhong Z, et al. Expanded sequence space of radical S-adenosylmethionine-dependent enzymes involved in post-translational macrocyclization. *Angew Chem Int Ed Engl*. 2022;61(48):e202212447. https://doi.org/10.1002/anie.202212447.
50 Oberg N, Precord TW, Mitchell DA, et al. RadicalSAM. org: a resource to interpret sequence-function space and discover new radical sam enzyme chemistry. *ACS Bio Med Chem Au*. 2022;2(1):22-35. https://doi.org/10.1021/acsbiomedchemau.1c00048.
51 Benjdia A, Guillot A, Ruffié P, et al. Post-translational modification of ribosomally synthesized peptides by a radical SAM epimerase in *Bacillus subtilis*. *Nat Chem*. 2017;9(7):698-707. https://doi.org/10.1038/nchem.2714.
52 Friedel MG, Berteau O, Pieck JC, et al. The spore photoproduct lyase repairs the 5*S*- and not the 5*R*-configured spore photoproduct DNA lesion. *Chem Commun (Camb)*. 2006;4:445-447. https://doi.org/10.1039/b514103f.
53 Chandor PA, Berteau O, Douki T, et al. DNA repair and free radicals, new insights into the mechanism of spore photoproduct lyase revealed by single amino acid substitution. *J Biol Chem*. 2008;283(52):36361-36368. https://doi.org/10.1074/jbc.M806503200.
54 Berteau O, Benjdia A. DNA repair by the radical SAM enzyme spore photoproduct lyase: from biochemistry to structural investigations. *Photochem Photobiol*. 2017;93(1):67-77. https://doi.org/10.1111/php.12702.
55 Morinaka BI, Vagstad AL, Helf MJ, et al. Radical S-adenosyl methionine epimerases: regioselective introduction of diverse D-amino acid patterns into peptide natural products. *Angew Chem Int Ed Engl*. 2014;53(32):8503-8507. https://doi.org/10.1002/anie.201400478.
56 Méjean A, Mazmouz R, Mann S, et al. The genome sequence of the cyanobacterium *Oscillatoria* sp. PCC 6506 reveals several gene clusters responsible for the biosynthesis of toxins and secondary metabolites. *J Bacteriol*. 2010;192(19):5264-5265. https://doi.org/10.1128/JB.00704-10.
57 Thiel T, Pratte BS, Zhong J, et al. Complete genome sequence of *Anabaena variabilis* ATCC 29413. *Stand Genomic Sci*. 2014;9(3):562-573. https://doi.org/10.4056/sigs.3899418.
58 Shih PM, Wu D, Latifi A, et al. Improving the coverage of the cyanobacterial phylum using diversity-driven genome sequencing. *Proc Natl Acad Sci U S A*. 2013;110(3):1053-1058. https://doi.org/10.1073/pnas.1217107110.
59 Pei ZF, Zhu L, Nair SK. Core-dependent post-translational modifications guide the biosynthesis of a new class of hypermodified peptides. *Nat Commun*. 2023;14(1):7734. https://doi.org/10.1038/s41467-023-43604-5.
60 Popp PF, Friebel L, Benjdia A, et al. The epipeptide biosynthesis locus epeXEPAB is widely distributed in *Firmicutes* and triggers intrinsic cell envelope stress. *Microb Physiol*. 2021;31(3):306-318. https://doi.org/10.1159/000516750.
61 Butcher BG, Lin YP, Helmann JD. The yydFGHIJ operon of *Bacillus subtilis* encodes a peptide that induces the liars two-component system. *J Bacteriol*. 2007;189(23):8616-8625. https://doi.org/10.1128/JB.01181-07.
62 Kubiak X, Polsinelli I, Chavas LMG, et al. Structural and mechanistic basis for RiPP epimerization by a radical SAM enzyme. *Nat Chem Biol*. 2024;20(3):382-391. https://doi.org/10.1038/s41589-023-01493-1.
63 Grillo MA, Colombatto S. S-adenosylmethionine and its products. *Amino Acids*. 2008;34(2):187-193. https://doi.org/10.1007/s00726-007-0500-9.
64 O'Hagan D, Schmidberger JW. Enzymes that catalyse SN2 reaction mechanisms. *Nat Prod Rep*. 2010;27(6):900-918. https://doi.org/10.1039/b919371p.
65 Yan F, LaMarre JM, Röhrich R, et al. RlmN and Cfr are radical SAM enzymes involved in methylation of ribosomal RNA. *J Am Chem Soc*. 2010;132(11):3953-3964. https://doi.org/10.1021/ja910850y.
66 Hu Y, Ribbe MW. Maturation of nitrogenase cofactor-the role of a class E radical SAM methyltransferase NifB. *Curr Opin Chem Biol*. 2016;31:188-194. https://doi.org/10.1016/j.cbpa.2016.02.016.
67 Nguyen TQ, Nicolet Y. Structure and catalytic mechanism of radical SAM methylases. *Life*. 2022;12(11):1732. https://doi.org/10.3390/life12111732.
68 Cheng J, Liu WQ, Zhu X, et al. Functional diversity of HemN-like proteins. *ACS Bio Med Chem Au*. 2022;2(2):109-119. https://doi.org/10.1021/acsbiomedchemau.1c00058.
69 Freeman MF, Helf MJ, Bhushan A, et al. Seven enzymes create extraordinary molecular complexity in an uncultivated bacterium. *Nat Chem*. 2017;9(4):387-395. https://doi.org/10.1038/nchem.2666.
70 Parent A, Guillot A, Benjdia A, et al. The B_{12}-radical SAM enzyme PoyC catalyzes valine C_{β}-methylation during polytheonamide biosynthesis. *J Am Chem Soc*. 2016;138(48):15515-15518. https://doi.org/10.1021/jacs.6b06697.
71 Huo L, Rachid S, Stadler M, et al. Synthetic biotechnology to study and engineer ribosomal bottromycin biosynthesis. *Chem Biol*. 2012;19(10):1278-1287. https://doi.org/10.1016/j.chembiol.2012.08.013.
72 Pierre S, Guillot A, Benjdia A, et al. Thiostrepton tryptophan methyltransferase expands the chemistry of radical SAM enzymes. *Nat Chem Biol*. 2012;8(12):957-959. https://doi.org/10.1038/nchembio.1091.
73 Benjdia A, Pierre S, Gherasim C, et al. The thiostrepton A tryptophan methyltransferase TsrM catalyses a Cob(II)Alamin-dependent methyl transfer reaction. *Nat Commun*. 2015;6:8377. https://doi.org/10.1038/ncomms9377.
74 Blaszczyk AJ, Knox HL, Booker SJ. Understanding the role of electron donors in the reaction catalyzed by Tsrm, a cobalamin-dependent radical S-adenosylmethionine methylase. *J Biol Inorg Chem*. 2019;24(6):831-839. https://doi.org/10.1007/s00775-019-01689-8.
75 Knox HL, Chen PT, Blaszczyk AJ, et al. Structural basis for non-radical catalysis by TsrM, a radical SAM methylase. *Nat Chem Biol*. 2021;17(4):485-

491. https://doi.org/10.1038/s41589-020-00717-y.
76 Ding W, Li Y, Zhao J, et al. The catalytic mechanism of the class C radical S-adenosylmethionine methyltransferase NosN. *Angew Chem Int Ed Engl*. 2017;56(14):3857-3861. https://doi.org/10.1002/anie.201609948.
77 Schinke C, Martins T, Queiroz SCN, et al. Antibacterial compounds from marine bacteria, 2010–2015. *J Nat Prod*. 2017;80(4):1215-1228. https://doi.org/10.1021/acs.jnatprod.6b00235.
78 Jin WB, Wu S, Xu YF, et al. Recent advances in HemN-like radical S-adenosyl-L-methionine enzyme-catalyzed reactions. *Nat Prod Rep*. 2020;37(1):17-28. https://doi.org/10.1039/c9np00032a.
79 Zhang Z, Mahanta N, Hudson GA, et al. Mechanism of a class C radical S-adenosyl-L-methionine thiazole methyl transferase. *J Am Chem Soc*. 2017;139(51):18623-18631. https://doi.org/10.1021/jacs.7b10203.
80 Mahanta N, Zhang Z, Hudson GA, et al. Reconstitution and substrate specificity of the radical S-adenosyl-methionine thiazole C-methyltransferase in thiomuracin biosynthesis. *J Am Chem Soc*. 2017;139(12):4310-4313. https://doi.org/10.1021/jacs.7b00693.
81 Repka LM, Chekan JR, Nair SK, et al. Mechanistic understanding of lanthipeptide biosynthetic enzymes. *Chem Rev*. 2017;117(8):5457-5520. https://doi.org/10.1021/acs.chemrev.6b00591.
82 Hudson GA, Burkhart BJ, DiCaprio AJ, et al. Bioinformatic mapping of radical S-adenosylmethionine-dependent ribosomally synthesized and post-translationally modified peptides identifies new Cα, Cβ, and Cγ-linked thioether-containing peptides. *J Am Chem Soc*. 2019;141(20):8228-8238. https://doi.org/10.1021/jacs.9b01519.
83 Babasaki K, Takao T, Shimonishi Y, et al. Subtilosin A, a new antibiotic peptide produced by *Bacillus subtilis* 168: isolation, structural analysis, and biogenesis. *J Biochem*. 1985;98(3):585-603. https://doi.org/10.1093/oxfordjournals.jbchem.a135315.
84 Lee H, Churey JJ, Worobo RW. Biosynthesis and transcriptional analysis of thurincin H, a tandem repeated bacteriocin genetic locus, produced by *Bacillus thuringiensis* SF361. *FEMS Microbiol Lett*. 2009;299(2):205-213. https://doi.org/10.1111/j.1574-6968.2009.01749.x.
85 Rea MC, Sit CS, Clayton E, et al. Thuricin CD, a posttranslationally modified bacteriocin with a narrow spectrum of activity against *Clostridium difficile*. *Proc Natl Acad Sci USA*. 2010;107(20):9352-9357. https://doi.org/10.1073/pnas.0913554107.
86 Sit CS, McKay RT, Hill C, et al. The 3D structure of thuricin CD, a two-component bacteriocin with cysteine sulfur to α-carbon cross-links. *J Am Chem Soc*. 2011;133(20):7680-7683. https://doi.org/10.1021/ja201802f.
87 Liu WT, Yang YL, Xu Y, et al. Imaging mass spectrometry of intraspecies metabolic exchange revealed the cannibalistic factors of *Bacillus subtilis*. *Proc Natl Acad Sci U S A*. 2010;107(37):16286-16290. https://doi.org/10.1073/pnas.1008368107.
88 Flühe L, Burghaus O, Wieckowski BM, et al. Two [4Fe-4S] clusters containing radical SAM enzyme SkfB catalyze thioether bond formation during the maturation of the sporulation killing factor. *J Am Chem Soc*. 2013;135(3):959-962. https://doi.org/10.1021/ja310542g.
89 Duarte AFDS, Ceotto VH, Barrias ES, et al. Hyicin 4244, the first sactibiotic described in Staphylococci, exhibits an anti-staphylococcal biofilm activity. *Int J Antimicrob Agents*. 2018;51(3):349-356. https://doi.org/10.1016/j.ijantimicag.2017.06.025.
90 Mo T, Ji X, Yuan W, et al. Thuricin Z: a narrow-spectrum sactibiotic that targets the cell membrane. *Angew Chem Int Ed Engl*. 2019;58(52):18793-18797. https://doi.org/10.1002/anie.201908490.
91 Chiumento S, Roblin C, Kieffer JS, et al. Ruminococcin C, a promising antibiotic produced by a human gut symbiont. *Sci Adv*. 2019;5(9):eaaw9969. https://doi.org/10.1126/sciadv.aaw9969.
92 Balty C, Guillot A, Fradale L, et al. Biosynthesis of the sactipeptide ruminococcin C by the human microbiome: mechanistic insights into thioether bond formation by radical SAM enzymes. *J Biol Chem*. 2020;295(49):16665-16677. https://doi.org/10.1074/jbc.RA120.015371.
93 Roblin C, Chiumento S, Bornet O, et al. The unusual structure of ruminococcin C1 antimicrobial peptide confers clinical properties. *Proc Natl Acad Sci U S A*. 2020;117(32):19168-19177. https://doi.org/10.1073/pnas.2004045117.
94 Bushin LB, Covington BC, Rued BE, et al. Discovery and biosynthesis of streptosactin, a sactipeptide with an alternative topology encoded by commensal bacteria in the human microbiome. *J Am Chem Soc*. 2020;142(38):16265-16275. https://doi.org/10.1021/jacs.0c05546.
95 Flühe L, Knappe TA, Gattner MJ, et al. The radical SAM enzyme AlbA catalyzes thioether bond formation in subtilosin A. *Nat Chem Biol*. 2012;8(4):350-357. https://doi.org/10.1038/nchembio.798.
96 Bruender NA, Wilcoxen J, Britt RD, et al. Biochemical and spectroscopic characterization of a radical S-adenosyl-L-methionine enzyme involved in the formation of a peptide thioether cross-link. *Biochemistry*. 2016;55(14):2122-2134. https://doi.org/10.1021/acs.biochem.6b00145.
97 Benjdia A, Guillot A, Lefranc B, et al. Thioether bond formation by SPASM domain radical SAM enzymes: C_α H-atom abstraction in subtilosin a biosynthesis. *Chem Commun (Camb)*. 2016;52(37):6249-6252. https://doi.org/10.1039/c6cc01317a.
98 Ding W, Li Y, Zhang Q. Substrate-controlled stereochemistry in natural product biosynthesis. *ACS Chem Biol*. 2015;10(7):1590-1598. https://doi.org/10.1021/acschembio.5b00104.
99 Grove TL, Himes PM, Hwang S, et al. Structural insights into thioether bond formation in the biosynthesis of sactipeptides. *J Am Chem Soc*. 2017;139(34):11734-11744. https://doi.org/10.1021/jacs.7b01283.
100 Caruso A, Bushin LB, Clark KA, et al. Radical approach to enzymatic β-thioether bond formation. *J Am Chem Soc*. 2019;141(2):990-997. https://doi.org/10.1021/jacs.8b11060.
101 Zorzi A, Deyle K, Heinis C. Cyclic peptide therapeutics: past, present and future. *Curr Opin Chem Biol*. 2017;38:24-29. https://doi.org/10.1016/j.cbpa.2017.02.006.
102 Clark KA, Seyedsayamdost MR. Bioinformatic atlas of radical SAM enzyme-modified RiPP natural products reveals an isoleucine–tryptophan crosslink. *J Am Chem Soc*. 2022;144(39):17876-17888. https://doi.org/10.1021/jacs.2c06497.
103 Caruso A, Martinie RJ. Macrocyclization *via* an arginine-tyrosine crosslink broadens the reaction scope of radical S-adenosylmethionine enzymes. *J Am Chem Soc*. 2019;141(42):16610-16614. https://doi.org/10.1021/jacs.9b09210.
104 Davis KM, Schramma KR, Hansen WA, et al. Structures of the peptide-modifying radical SAM enzyme SuiB elucidate the basis of substrate recognition. *Proc Natl Acad Sci U S A*. 2017;114(39):10420-10425. https://doi.org/10.1073/pnas.1703663114.
105 Balo AR, Caruso A, Tao L, et al. Trapping a cross-linked lysine–tryptophan radical in the catalytic cycle of the radical SAM enzyme SuiB. *Proc Natl Acad Sci U S A*. 2021;118(21):e2101571118. https://doi.org/10.1073/pnas.2101571118.
106 Clark KA, Bushin LB, Seyedsayamdost MR. Aliphatic ether bond formation expands the scope of radical SAM enzymes in natural product biosynthesis. *J Am Chem Soc*. 2019;141(27):10610-10615. https://doi.org/10.1021/jacs.9b05151.
107 Hug JJ, Dastbaz J, Adam S, et al. Biosynthesis of cittilins, unusual ribosomally synthesized and post-translationally modified peptides from *Myxococcus xanthus*. *ACS Chem Biol*. 2020;15(8):2221-2231. https://doi.org/10.1021/acschembio.0c00430.
108 Zdouc MM, Alanjary MM, Zarazúa GS, et al. A biaryl-linked tripeptide from Planomonospora reveals a widespread class of minimal RiPP Gene clusters. *Cell Chem Biol*. 2021;28(5):733-739.e4. https://doi.org/10.1016/j.chembiol.2020.11.009.
109 Greule A, Izoré T, Iftime D, et al. Kistamicin biosynthesis reveals the biosynthetic requirements for production of highly crosslinked glycopeptide antibiotics. *Nat Commun*. 2019;10(1):2613. https://doi.org/10.1038/s41467-019-10384-w.
110 Li X, Ma S, Zhang Q. Chemical synthesis and biosynthesis of darobactin. *Tetrahedron Lett*. 2023;116:154337. https://doi.org/10.1016/j.tetlet.2023.154337.
111 Ma S, Guo S, Ding W, et al. Daropeptide natural products. *Explor Drug Sci*. 2024;2:190-202.
112 Nguyen H, Made Kresna ID, Böhringer N, et al. Characterization of a radical SAM oxygenase for the ether crosslinking in darobactin biosynthesis. *J Am Chem Soc*. 2022;144(41):18876-18886. https://doi.org/10.1021/jacs.2c05565.
113 Ma S, Xi W, Wang S, et al. Substrate-controlled catalysis in the ether cross-link-forming radical SAM enzymes. *J Am Chem Soc*. 2023;145(42):22945-22953. https://doi.org/10.1021/jacs.3c04355.
114 Bushin LB, Covington BC, Clark KA, et al. Bicyclostreptins are radical SAM enzyme-modified peptides with unique cyclization motifs. *Nat Chem Biol*. 2022;18(10):1135-1143. https://doi.org/10.1038/s41589-022-01090-8.
115 Nguyen TQN, Tooh YW, Sugiyama R, et al. Post-translational formation of strained cyclophanes in bacteria. *Nat Chem*. 2020;12(11):1042-1053. https://doi.org/10.1038/s41557-020-0519-z.
116 Zhu W, Walker LM, Tao L, et al. Structural properties and catalytic implications of the SPASM domain iron–sulfur clusters in *Methylorubrum extorquens* PqqE. *J Am Chem Soc*. 2020;142(29):12620-12634. https://doi.org/10.1021/jacs.0c02044.
117 Ma S, Chen H, Li H, et al. Post-translational formation of aminomalonate by a promiscuous peptide-modifying radical SAM enzyme. *Angew Chem Int Ed Engl*. 2021;60(36):19957-19964. https://doi.org/10.1002/anie.202107192.
118 Zhu W, Iavarone AT, Klinman JP. Hydrogen-deuterium exchange mass spectrometry identifies local and long-distance interactions within the multicomponent radical SAM enzyme, PqqE. *ACS Cent Sci*. 2024;10(2):251-263. https://doi.org/10.1021/acscentsci.3c01023.
119 Booker SJ, Lloyd CT. Twenty years of radical SAM! The genesis of the superfamily. *ACS Bio Med Chem Au*. 2022;2(6):538-547. https://doi.org/10.1021/acsbiomedchemau.2c00078.

Xinya Hemu: a professor at the School of Traditional Chinese Pharmacy at China Pharmaceutical University (since 2022). She received her Ph.D. with a focus on peptide ligation chemistry in 2014 at Nanyang Technological University and continued post-doctoral research on the design and biosynthesis of bioactive peptides. Her research interests focus on the discovery and redesign of peptide ligases for peptide and protein engineering and the computer-assisted design of peptidyl therapeutics. She has published more than 30 papers on SCI journals including JACS and PNAS, with over 1000 citations.